Influence of Material Doping Degree on Performance of IMCCR Used for EV

Cao Junci[1,2], Li Weili[2], Zhang Yihuang[1], Huo Feiyang[1]
[1]School of Electrical Engineering, Beijing Jiaotong University Beijing 100044, China
[2]School of Electrical and Electronic Engineering, Harbin University of Science and Technology, Harbin, 150040, China
E-mail: caojunci@163.com, li.weili@yeah.net

Abstract- **At present, the total or main power energy in plug-in hybrid electrical vehicles and electrical vehicles is a limited energy source, and reducing the unnecessary loss effectively becomes one of the methods to enhance vehicle efficiency. In this paper, a kind of induction motor with compound cage rotor(IMCCR) is proposed, in which rotor bars are composed of upper parts made of alloy (conductor for electric and magnetic) and lower parts made of cast aluminum. By using FEM, starting performances of IMCCR is studied. From the comparison of obtained results with the test data, it can be inferred that IMCCR would be a better choice for driving system in vehicles. Considering the variation of alloy material characteristics caused by different materials components doping degrees, the influences of alloy bar materials on IMCCR flux distribution and machine performance are studied. Meanwhile, the effects special alloy bar positions and numbers on machine starting performance are researched. Some conclusions are summarized, which may provide useful reference for improving on driving induction motors used for vehicles.**

I. INTRODUCTION

Electric vehicles (EV) become the further development direction of vehicles industry for its favorable features. Although battery is very important to electric vehicles, the driving motor is significant too, and the major types of electric motors adopted for EVs are the permanent magnet motors [1] and the induction motors [2-4]. The driving motor should have excellent acceleration torque to satisfy EV requests in starting, accelerating and climbing, and also should with high efficiency. So how to increase starting torque and decrease starting current, without affecting motor efficiency and power factor become an actual problem for motors used in vehicles driving system[5].

In this paper, a kind of induction motor with compound cage rotor (IMCCR) is proposed, whose stator structure is the same as that of the traditional induction motor, whereas rotor bars are composed of two parts. The upper one is made of alloy (conductor for electric and magnetic), by which motor starting performance is improved, and lower part is made of cast aluminum to ensure motor operating performance. While used in EVs or PHEVs, the rational designed IMCCR could reduce the capacity of matched frequency variation system dramatically, and improve the efficiency of battery and driving system practically [6-7]. Therefore, the research work on IMCCR performances while working in vehicles would be meaningful.

According to [8-10], most study work for rotor materials in caged induction motor focus on the electrical and mechanical properties. Most materials are difficult to be practically used widely for the reasons of manufacture and cost, and also it is difficult to determine the ratio of different kinds of metals in alloy which influences its performance very much. Furthermore, for the doping ratio and manufacture reasons, the materials may distribute not evenly in alloy, which would affect rotor bar properties, even the performance of motor and driving system in vehicles.

In this paper, the starting performance of IMCCR is studied and the influence of alloy material on motor performance is investigated. While the material characteristics of a single alloy bar and continuous two bars in rotor cage are changed, the variations of motor flux distribution and performance are studied under the same conditions. Thus, the influence of material doping degree on IMCCR performance is researched, which may provide reference for optimization design of this kind of motor.

II. INTRODUCTION

IMCCR, a type of induction motor with improved rotor structure and material, is proposed based on structure and characteristics study of normal squirrel cage induction motor and solid rotor induction motor. In the motor, stator slot type and windings are similar to that of normal induction motor, and bar shape and material in rotor cage are redesigned, which is shown in Fig.1.

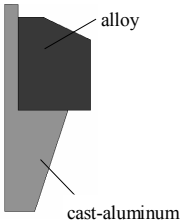

Fig. 1. Outline of rotor slot and bars.

In the motor proposed here, rotor slot shape and bar material work together to improved motor performance. As that of double-squirrel cage induction motor, the upper alloy bars and lower aluminum bars are two different electricity conductance layers. Considering that starting cage (upper cage) is made of alloy and operating cage (lower cage) is made of cast aluminum, the equivalent circuit of IMCCR could be shown as Fig.2. While starting, alloy bars strengthen

978-1-4244-8218-4/10/$26.00 ©2010 IEEE

the Kelvin effect, which would improve motor starting performance, whereas aluminum bars plays the leading role while operating to make IMCCR has the same operating performance as normal induction motor. Thus it can be estimated that IMCCR could have high starting performance as solid rotor induction motor, and similar operating performance to normal induction motor, which would satisfy the requests of EV driving system, also may expand applications of this kind of motor in other fields [12].

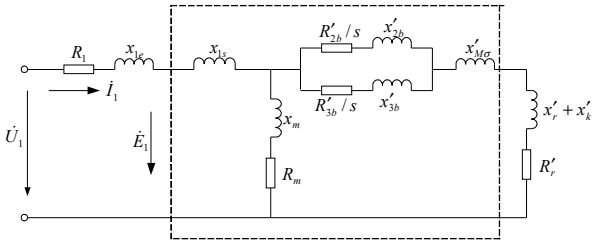

Fig. 2. Equivalent circuit of IMCCR.

A 3kW prototype of IMCCR is produced and tested. The experiment equipments are shown in Fig.3. Here, magnetic powder brake is selected as the simulation load. The input parameters are tested by HIOKI 3166 Clamp on Power Hi-Tester, and the output parameters of IMCCR are measured by the torque and speed sensor (JW-2A) that co-axial connected with magnetic powder brake and motor shaft. The temperature inside motor is monitored by heat sensitive resistance with precision of 0.1℃.

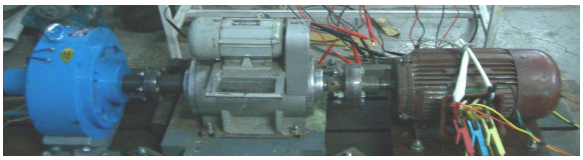

Fig. 3. Experimental setup for IMCCR.

III. ANALYSIS OF ELECTROMAGNETIC FIELD

To simplify the analysis during the electromagnetic analysis process, following assumptions are proposed [11-12]:

(a)For air-gap length is so small compare with motor polar pitch that the distribution of magnetic density or flux is considered invariable along the axial direction. Within the core length, magnetic field distribution in motor core would be two-dimensional (2-D) perpendicular to axial direction.

(b)Kelvin effect in stator core and windings are ignored.

(c)Flux density, magnetic intensity and magnetic vector potential are sinusoidal wave with time.

Based on assumptions above, the whole cross-section region of motor core perpendicular to axial direction (z-axial) is selected as the 2-D analysis model, as shown in Fig.4.

For the whole cross section of the motor is taken as the calculation region, at the boundary of stator outer periphery (s_1) and rotor inner periphery (s_2) $\dot{A}_z = 0$. According to [11], the boundary value for electromagnetic analysis would be

$$\left.\begin{aligned} &\frac{\partial}{\partial x}\left(\frac{1}{\mu_e}\frac{\partial \dot{A}_z}{\partial x}\right)+\frac{\partial}{\partial y}\left(\frac{1}{\mu_e}\frac{\partial \dot{A}_z}{\partial y}\right)=js\omega\sigma\dot{A}_z-\dot{J}_z \\ &\dot{A}_z\mid_{s=s_1+s_2}=0 \end{aligned}\right\} \tag{1}$$

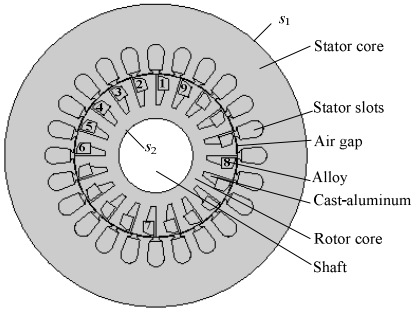

Fig. 4. Structure and calculation model of IMCCR.

In the analysis of 2D electromagnetic field only core length range of motor is considered effectively (dotted-line box in Fig.2), and other parts should be involved in some parameters. Here, rotor end-ring resistance R'_{2r} and end-ring leakage reactance x'_{2r} are considered together with bar resistance R'_{2b} and slot leakage reactance x'_{2s}, respectively. Therefore, rotor bar conductivity and permeability are modified by flowing equations, respectively [12].

$$\sigma' = \sigma\frac{R'_{2b}}{R'_{2b}+R'_{2r}}, \quad \mu'_b = \mu_b\frac{x'_{2s}+x'_{2r}}{x'_{2s}} \tag{2}$$

The detailed calculation process is as following. First, the element mesh is carried on, and an initial current under rated voltage is given (the initial value is estimated from the traditional magnetic circuit calculation). Then, source current density value and the initial effective magnetic permeability are applied. By using FEM, the magnetic is calculated numerically

Beside the FEM calculation, there are two convergence processes too. One is stator current convergence and the other is slip convergence, which take rated terminal voltage and rated output power as the convergence requests, respectively. The stator current and slip iterations are carried out synchronously, and are modified as linear relation by (3) and (4), respectively. Until the calculated voltage and out-put power are satisfying all the requirements, this calculation would be done repeatedly.

$$\left.\begin{aligned} &\dot{U}=\dot{I}(R_1+jx_{1e})-\dot{E} \\ &I_m^{(k)}=I_m^{(k-1)}\frac{U}{U^{(k-1)}} \end{aligned}\right\} \tag{3}$$

where $\dot{U}$ is stator terminal voltage, $\dot{E}$ is stator phase electromotive force, R_1 and x_{1e} are stator winding resistance and leakage reactance, respectively.

$$\left.\begin{aligned} P_e &= P_{cu2} + P_\Omega + P_s + P_2 \\ s^{(k)} &= s^{(k-1)} \frac{P_2}{P_2^{(k-1)}} \end{aligned}\right\} \quad (4)$$

where P_e is electromagnetic power, P_{cu2} is rotor bar loss, P_Ω is mechanical loss, P_s is stray loss and P_2 is output power.

The flux distribution of motor while starting is shown in Fig.5, from which we can see that the field distribution is very complex, and Kelvin effect in rotor is obviously. Most of the rotor flux through upper alloy bars in rotor slots, thus this magnetic conductive alloy material promotes Kelvin effect become strong, and improve motor starting performance significantly.

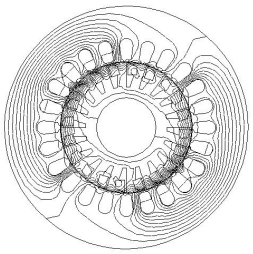

Fig. 5. Flux distribution of IMCCR while starting.

After some associated test work, Tab.I shows the comparison of this prototype starting performance with that of same power induction motor. Under the same conditions, starting current of IMCCR is 13.4% smaller than that of normal induction motor, whereas starting torque is about 5% bigger. Therefore, the good starting performance of IMCCR could be clearly.

TABLE I
TYPE SIZES FOR CAMERA-READY PAPERS COMPARISON OF MOTOR STARTING PERFORMANCE

	IMCCR		Normal induction motors
	Calculated	Test	Test
Starting current(A)	33.69	34.1	38.9
Starting torque(N·m)	23.68	23.7	21.6

IV. INFLUENCES OF MATERIALS DOPING DEGREES ON IMCCR PERFORMANCE

The alloy is mainly composed of industrial pure iron (81.7% in weight) and electrolytic copper (17% in weight). For deoxidizing and forming, some trace elements, such as Manganese, Phosphorus, Aluminum, Magnesium, etc., are added to the alloy through casting. From an associate test, the permeability of the alloy (μ_a) is about 20 times than that of air, and its electric resistivity (ρ_a) is about 0.67 times than that of iron.

In the process of alloy materials production, if composite materials fusion is melted not completely or mixed unevenly, the material doping degree in alloy bars may different, which would affect its properties, even the performance of IMCCR. If the main materials component proportions in alloy changed, the conductivities of alloy in magnetic and electric are changing with the same trend, and the changing proportions depend on the materials characteristics and its proportion accounts in alloy. Considering the materials properties variation caused by different materials doping degrees, the performances of several IMCCRs with different cage bars are calculated separately, in which alloy bar materials with the resistivity is within 50%-135% ρ_a and permeability is within 50%-135% μ_a.

A. Influence of single alloy bar material variation on motor starting performance

For this analysis focus on the motor starting performance variation caused by material properties change in a single alloy rotor bar, the initial locations of this bar corresponding to stator may affect motor starting performance. In this paper, the starting performance of IMCCR with such an alloy cage bar locates at No.1-No.8 slots (as shown in Fig.4) are analyzed, respectively. Tab.II shows the starting torque variation when the alloy bar locates at different positions with material resistivity decrease to 50% ρ_a, in which the biggest starting torque difference among different special alloy bar positions is only 0.24%, which could be ignored. Thus, in the following studies, only special alloy bar at No.1 slot is considered.

TABLE II
COMPARISON OF STARTING TORQUE OF IMCCR WITH SPECIAL ALLOY BAR AT DIFFERENT POSITIONS

Positions	1	2	3	4	5	6	7	8
Starting torque (N·m)	23.277	23.307	23.224	23.222	23.263	23.256	23.278	23.256
Difference	0	0.128%	0.227%	0.237%	0.05%	0.092%	0.002%	0.092%

By using FEM composed with terminal voltage iteration, starting performances of IMCCR are analyzed while material properties of alloy bar at No.1 slot changes. When meeting the same convergence requests of motor voltage (0.5%), the variation of obtained stator starting current with alloy bar material is so slightly (0.012A) that the influence of single alloy bar material doping degree on motor stator current could be ignored, which could be clearly in Fig.6a). Whereas for motor starting torque, the effect caused by material is bigger. Fig.6b) presents the variation curve of motor starting torque with material properties of alloy bar at No.1 slot, in which motor torque increases nonlinearly with alloy bar resistivity. While alloy resistivity changes in the region of 50%-135% ρ_a, the incremental of motor starting torque is about 0.55 N·m, which is about 2.32% of the normal value.

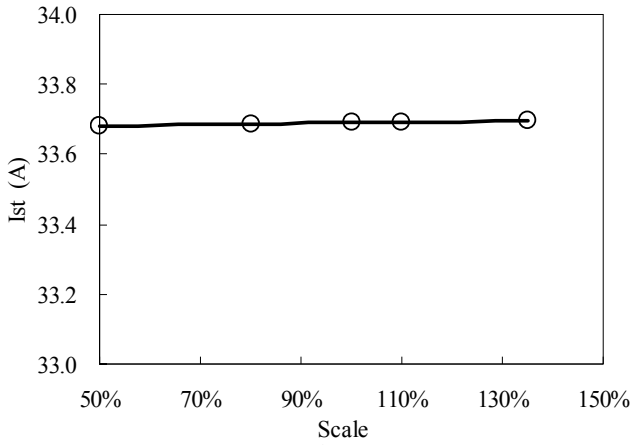

a) Starting current

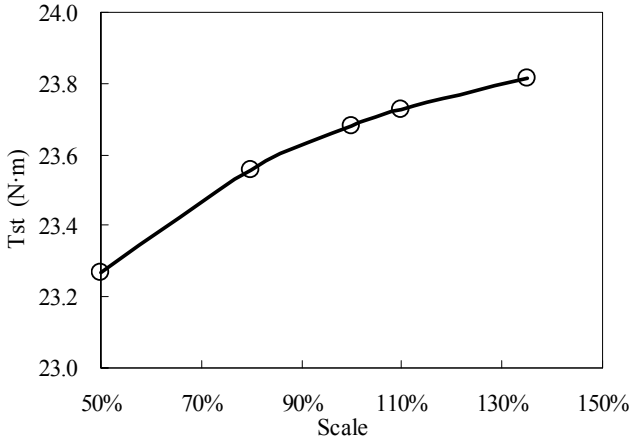

b) Starting torque

Fig. 6. Variation of motor starting performance with material of one alloy bar.

Through the FEM numerical analysis, it could be indicated that the variation of material properties in a single alloy cage motor bar has little influence on the overall distribution of vector magnetic potential, but certain affection on the local position, especially for the bar whose material properties changed. Fig.7 shows flux distributions in alloy bar at No.1 slot with different material properties, in which the magnetic densities at notches are much bigger because of the Kelvin effect, which may cause high eddy current density.

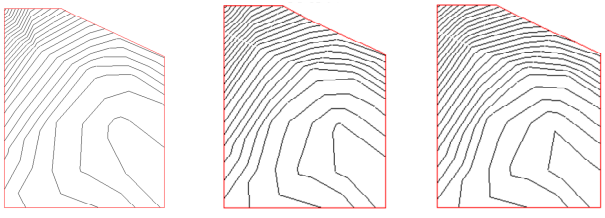

a) 50% b) 100% c) 135%

Fig. 7. Flux distributions in alloy bars with different material properties.

While starting, rotor tooth top is in high saturation state, and the high flux density at these locations interest many scholars and motor designers. Although the variation of material properties affects vector magnetic potential distribution in some degree, is has little influence on flux density. Just as shown in Fig.8, the variation curve of average magnetic density at rotor teeth top with alloy bar material is nearly a straight line.

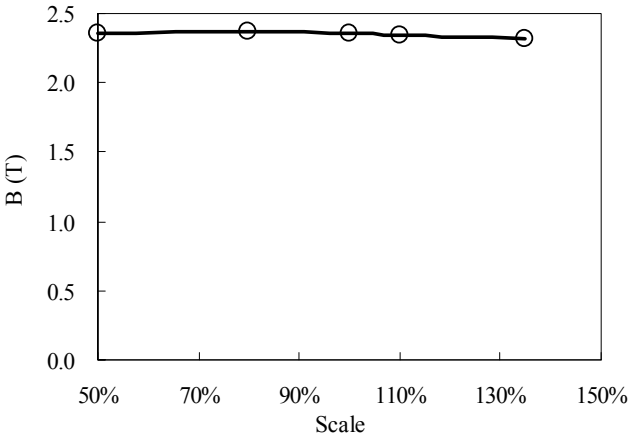

Fig. 8. Variation of average flux density at tooth top with alloy bar material.

The change of bar resistivity may lead to the variation of induced eddy current in it, even the eddy loss. As the rise of alloy material resistivity, the eddy current density decrease gradually, as shown in Fig. 9, and the eddy loss in it is also reducing gradually. Fig.10 shows the eddy loss variation trend of alloy bar at No.1 slot with its resistivity.

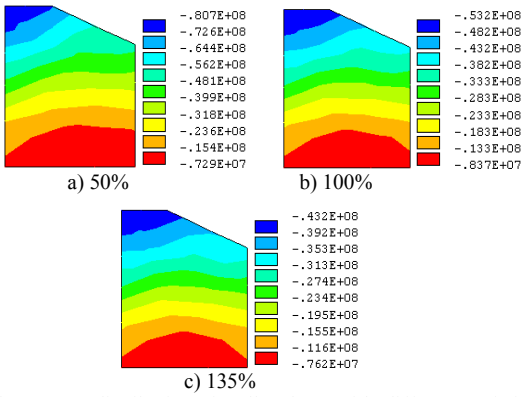

a) 50% b) 100%

c) 135%

Fig. 9. Eddy current distributions in alloy bars with different resistivity (A/m^2).

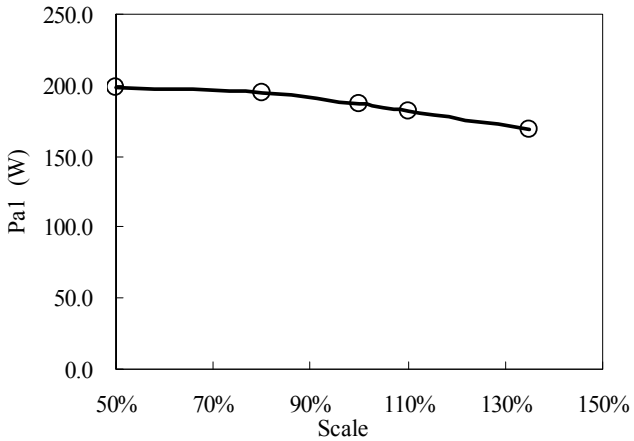

Fig. 10. Variation of eddy loss in alloy bar with its resistivity.

To analyze the influence of alloy material variation on other rotor bar, the bar next to No.1 slot are analyzed (No.2 and No.9 slots at left and right of No.1, respectively). The variation curves of losses in bars in No.2 and No.9 slots are shown in Fig.11. Opposite to that in Fig.8, losses in the bars are increasing correspondingly with alloy resistivity of bar in No.1 slot, also the torques produced by these bars. Thus, although the eddy current in bar at No.1 slot is reducing the total starting torque is increasing.

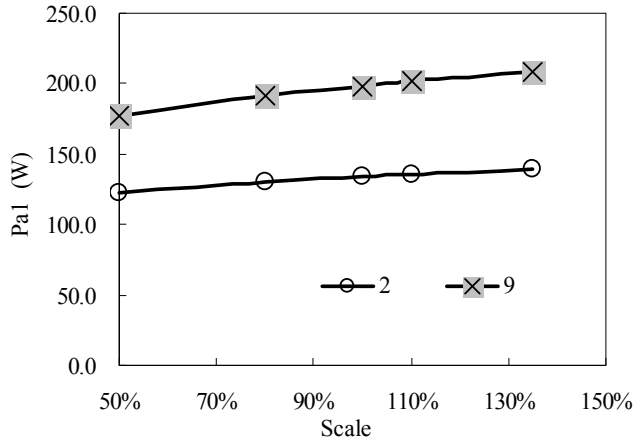

Fig. 11. Variation of eddy losses of alloy bars in No.2 and No.9 slots.

B. Influence of continuous two alloy bars material variation on motor starting performance

Based on above analysis, IMCCR starting performances while rotors with two continuous alloy bars material changed are analyzed. In the studied, the two bars located at No.1 and No.2 slot (position A), and at No.1 and No.9 slot (position B) are analyzed, respectively, whose material doping degree variations are considered.

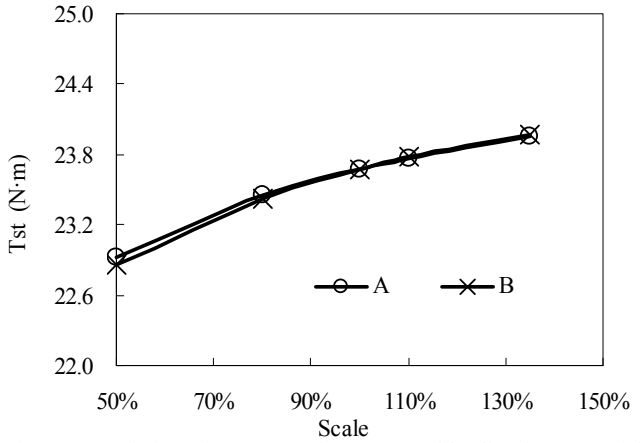

Fig. 12. Variation of motor starting torque with alloy bars material at positions A and B.

Fig.12 shows the variation curves of motor starting torque as two continuous bar material properties changing. Comparing to that of single bar material changed, under same terminal voltage, motor starting current decreases slightly, which is about 0.1% less than normal ones while special bars at position A, and 0.035% while at position B. As rising of alloy resistivity and permeability, motor starting torque increase more obviously. It has increased about 4.35% and 4.73% while the bar at position A and B with material changes in 50% -135%.

CONCLUSIONS

(1)A type of induction motor IMCCR suits for using in vehicles is proposed. The IMCCR has high starting torque and low starting current which could be seen from the electromagnetic analysis and test.

(2)While the alloy bar with different material properties at different position corresponding to stator, starting current of IMCCR has little variation.

(3)As the rising of resistivity and permeability of a single bar, motor starting torque is increasing, nonlinearly.

(4)When the material properties of continuous two alloy bar is changed, motor starting torque increases more obviously. In the study, while special alloy bars at position A and position B, motor starting torque rises about 4.35% and 4.73%, respectively.

ACKNOWLEDGMENT

This work was supported in part by the National Natural Science Fund of China under Grant 50907015.

REFERENCES

[1] K. T. Chau, C. C. Chan, and Chunhua Liu. “Overview of Permanent-Magnet Brushless Drives for Electric and Hybrid Electric Vehicles,” *IEEE Trans. Ind. Electron.*, vol. 55, no. 6, pp. 2246-2257, Jun 2008.

[2] Jinhwan Jung and Kwanghee Nam. “A Vector Control Scheme for EV Induction Motors with a Series Iron Loss Model,” *IEEE Trans. Ind. Electron.*, vol. 45, no. 4, pp. 617-624, Aug 1998.

[3] Tiecheng Wang, Ping Zheng, Qianfan Zhang, and Shukang Cheng, “Design characteristics of the induction motor used for hybrid electric vehicle,” *IEEE Trans. Magn.,* vol. 41, no. 1, pp. 505-508, Jan 2005.

[4] Dong-Hyeok Cho, Hyun-Kyo Jung, and Cheol-Gyun Lee, “Induction motor design for electric vehicle using a niching genetic algorithm,” *IEEE Trans. Ind. Appl.*, vol. 37, no. 4, pp. 994–999, Jul 2001.

[5] Dejun Yin, Sehoon Oh, and Yoichi Hori, “A Novel Traction Control for EV Based on Maximum Transmissible Torque Estimation”, *IEEE Trans. Ind. Electron.,* vol. 56, no. 6, pp.2086-2094, Jun 2009.

[6] L. Weili, C. Junci and Z. Xiaochen, “Electro-thermal Analysis of Induction Motor with Compound Cage Rotor Used for PHEV,” *IEEE Trans. Ind. Electron.*, vol. 57, no. 2, pp. 660-668, Feb 2010.

[7] G. Dong, and O. Ojo., “Efficiency optimizing control of induction motor using natural variables”, *IEEE Trans. Ind. Electron.*, vol. 53, no. 6, pp. 1791-1798, Dec 2006.

[8] J. H. Dymond and R. D. Findlay, “Some commentary on the choice of rotor bar material for induction motors,” *IEEE Trans. Energy Conv.*, vol. 10, no. 3, pp. 425-430, Sep 1995.

[9] E. R. Mognaschi, J. H. Calderwood, “Significance of the time constant of the rotor material employed in a dielectric motor,” *International Journal of Applied Electromagnetics and Mechanics*, vol. 10, no. 2, pp. 177-183, Jan 1999.

[10] Y. P. Zhang, “The study on the modification of new material used for high slip and special three phase asynchronous motor rotors,” *Proceeding of the CSEE*, vol. 21, no. 8, pp. 89-93, Aug 2001.

[11] T. Yunqiu, *Electromagnetic Field in Electric Machine*. 2ed edition, Beijing: Science Press, 1998, pp. 273-279.

[12] Weili Li, Ying Xie, Jiafeng Shen and Yingli Luo. “Finite-Element Analysis of Field Distribution and Characteristic Performance of Squirrel-Cage Induction Motor with Broken Bars,” *IEEE Trans. Mag.*, vol. 43, no. 4, pp. 1537-1540, Apr 2007.